Bioinfo-pharmacology: the example of therapeutic hypothermia

Fei Liu[1,2,3,#]; Xiangkang Jiang[1,2,3], Mao Zhang[1,2,3,*]

Author affiliations:

1. Department of Emergency Medicine, Second Affiliated Hospital of Zhejiang University, Hangzhou 310009, Zhejiang Province, China.

2. Institute of Emergency Medicine, Zhejiang University, Hangzhou 310009, Zhejiang Province, China.

3. Key Laboratory of The Diagnosis and Treatment of Severe Trauma and Burn of Zhejiang Province, Zhejiang University, Hangzhou 310009, Zhejiang Province, China.

[#] The first 1 author is the first author.

* corresponding author: Prof. Mao Zhang

Email: z2jzk@zju.edu.cn

Telephone: +86 13757119125

Declaration

Ethics approval and consent to participate.

Not applicable.

Consent for publication

All authors allow the publication of this article.

Availability of data and materials

All the data that support the findings of this study are available for email from authors.

Competing interests

The authors have declared that they have no conflicts or interests.

Funding

The authors have stated that no such relationships exist.

Authors' contributions

MZ designed the research. XJ drew the pictures. FL wrote the article and analyzed the data.

Acknowledge

We thank Prof. Mu Li for algorithm consulting.

Abstract

Computer-aided drug discovery (CADD) is a widely used method for drug discovery with many successes. Meanwhile, CADD has the limitation of analyzing multi-level scores such as docking results of multiple proteins with multiple drugs. We propose a method of PageRank to solve the problem. This method can make a comprehensive ranking based on multi-level scores. Then we take an example of therapeutic hypothermia (TH). Three levels of TH data were used in the article: the log2 foldchange (logFC) of proteins, the relative expression values of mRNA, and the docking scores of proteins and molecules. After calculation, we get the comprehensive drug rank and drug combination rank of each group of TH, which means we can generate the rank of drug directly from bioinformatics. Based on this method, we raised the concept of bioinfo-pharmacology. Given the high rationality and compatibility of bioinfo-pharmacology, it can effectively enhance popular drug discovery techniques such as the docking or pharmacophore model. Besides, it could advance the application of precision medicine.

Keyword: computer-aided drug discovery (CADD); precision medicine; Therapeutic hypothermia; di□erential gene expression; virtual screening;

Introduction

Drug discovery is an expensive and time-demanding process that faces many challenges, including low hit discovery rates for high-throughput screening, among many others.(*1*, *2*) Methods of computer-aided drug discovery (CADD) can significantly speed up the pace of such screening and reduce the cost.(*3–5*) Until now, CADD has achieved important results. (*6–8*)

Meanwhile, CADD also has limitations. With the development of artificial intelligence, especially AlphaFold2(*9*) and RoseTTAFold(*10*), we can obtain the three-dimensional structure of proteins more quickly and accurately. However, CADD technologies can only analyze the binding of a single target or single molecular(*11*). Researchers can only get the best match for a particular target (drug development), or the best match for a particular molecule (network pharmacology(*12*)). As a result, most pharmacological studies currently work on a single target. However, according to bioinformatics databases, diseases/treatments exist multiple targets, which generate complex regulation functions, in the different stages of diseases/treatments.(*13*) So, if the CADD data can be further analyzed through comprehensive ranking among multi-targets or drugs, it will theoretically improve the treatment of drugs and advance the pharmacological theory.

Take therapeutic hypothermia as an example. At present, therapeutic hypothermia (TH) can limit the degree of some kind of injuries in randomized trials(*14*) and animal experiments(*15*), and is even the only effective method for some diseases especially hypoxic-ischemic encephalopathy (HIE). HIE often causes severe neurological

sequelae, which is the main reason for the poor prognosis of patients with stroke, shock, carbon monoxide poisoning, cerebral hemorrhage, and cardiac arrest.(*16–18*)

In the research based on TH, in addition to temporal differences in protein expression, there are also functional differences caused by spatial differences of proteins. Cold shock proteins especially Cold-induced RNA binding protein (CIRP) show high expression (*19*) and rapid response (*20*). CIRP has been suggested to be important for 3' end cleavage and polyadenylation, as well as for regulating translation of specific mRNAs helping the cell to adapt to cold stress(*21*). CIRP has been shown to promote the translation of genes involved in DNA repair (*22*, *23*), cellular redox metabolism(*24*), cellular adhesion(*25*), circadian homeostasis(*26*), reproduction(*27*), telomerase maintenance(*28*), and genes associated with the translational machinery(*29*).

However, if CIRP is leaked to the intercellular substance with cell swelling and rupture, it will become a strong pro-inflammatory substance. In different animal or cell models, extracellular CIRP (eCIRP) showed a strong pro-inflammatory effect, leading to a heavier hypoxic injury.(*30*, *31*) because of the habit of clinical medication, we cannot determine whether there are drugs that affect the therapeutic effect before and after the beginning of TH.

To solve the complex function differences by temporal and spatial distribution differences of proteins, we use PageRank to rank drugs targeting proteins predicted by newly published artificial intelligence technologies (AlphaFold2 and RoseTTAFold) at different groups to predict the best drugs or drug combinations for each group.

Based on these, we came up with the concept of bioinfo-pharmacology.

Methods

Experiment design

As shown in Figure 1, the representative experiment of bioinfo-pharmacology is divided into 5 processes:

1. Protein or mRNA expression obtained by bioinformatics analysis;
2. Protein and drugs 3D structure acquisition and prediction;
3. Proteins' active sites prediction;
4. Drug/molecular group evaluation with target proteins;
5. PageRank of docking results, protein logFC, and mRNA expression.

The experiment of animals or cells is referred by authors, but not forced.

The data source of bioinformatics analysis

We retrieved the original data of mRNA expression under hypothermia treatment from the website of The National Center for Biotechnology Information (NCBI) (GSE54229). The research was performed by Sten et.al.(*20*) In their research, mouse embryonic fibroblasts were exposed to mild hypothermia (32°C) or normothermia (37°C) to gain the transcription response induced by hypothermia. It was identified that the genes with time-dependent monotonic response were the most obvious candidate gene for the effect of TH.

Hypothermia Expression Profile Analysis

All hypothermia data were grouped by time points, and log2 fold-change (log2FC) and p-value were calculated for the normothermia group. Top 3 log2FC mRNA with q-value < 0.05 were selected from each group to enter the next step. If there exists

mRNA with failed protein structure prediction, the mRNA would be skipped.

R 3.6.1 (“affy”(*32*), “dendextend”(*33*)) was used to detect di erential expressed compared to matched normothermia samples. The clustering of genes was calculated by the “dist” and “hclust” function of R. The visualization of gene expression and clustering is performed by the “dendextend” package(*33*).

3D Data of proteins and small molecular drugs

3D Data of proteins and small molecular drugs

All proteins were first searched on PubMed to see if there was protein clipping like cleaved caspase-3(*34*).

Then the 3D structures of proteins were firstly retrieved from Research Collaboratory for Structural Bioinformatics Protein Data Bank (RCSB PDB, https://www.rcsb.org/), which is used for biological-related ligand-protein interaction. In this article, no protein structure is listed on the PDB website. So, all the protein structures were predicted by AlphaFold2(*9*) and RoseTTAFold(*10*).

AlphaFold2 is developed by Google and is the champion of the 14th Critical Assessment of Structure Prediction (CASP14)(*35*). In August 2021, AlphaFold submitted a structure prediction database for all proteins. It changed workflows in structural biology.(*36*) RoseTTAFold is based on the Rosetta software which is designed for macromolecular modeling, docking, and design is extensively used in laboratories worldwide.(*37*) RoseTTAFold also has good application(*38*) in research of protein structure prediction. Finally, protein structures having a relatively regular structure and having fewer irregular regions will be selected for the next step.

The 3D structure data of 8,697 drugs (DrugBank Release Version 5.1.8) were downloaded from DrugBank Online(*39*) (https://go.drugbank.com/). Approved, experimental, nutraceutical, and investigational drugs by Food and Drug Administration (FDA) are included. The original data was a single file of all drugs in SDF format. We split each drug molecule into a PDBQT-format file and minimized the energy separately for docking with proteins.

Visualize evolutionary conservation and active site prediction

Visualize evolutionary conservation was performed by ConSurf server(*40*). In a typical ConSurf application, through BLASTed(*41*) against the UNIREF-90 database(*42*) and aligning using MAFFT(*43*), the evolutionarily conserved of positions are analyzed by Rate4Site algorithm(*44*).

Then, Consensus approach-D (COACH-D) (*45*, *46*) was used to predict the active site of target proteins. The progress of COACH-D is as follows: 1. I-TASSER Kit(*47*) was used to simulate the 3D protein structure. 2. The simulated structure was submitted to five different methods to predict the binding sites of protein ligands. Four of these methods are COFAC-TOR(*48*), FINDSITE(*49*), TM-SITE(*45*), and S-SITE(*45*). These methods predict binding sites by matching the query structure and sequence with the ligand-binding template in BioLiP(*50*), which is a semi-manual functional database(*51*) based on the PDB. The last one is based on the concave method of template-free structure, which is used to predict binding sites by analyzing both sequence conservation and structural geometry(*52*). 3. The results of each method are combined into consistency prediction by the algorithm. Detailed descriptions of these methods are provided in the publications of the original algorithm(*45*) and the corresponding methods(*48*, *49*, *52*). 4. Finally, ligands from user input or template are

connected to predicted vesicles by AutoDock Vina(*53*), and their complex structures are constructed. For each predicted bandage bag, a maximum of ten bandage positions are generated and the most matching position with the consistent predicted bandage residue is selected.

Virtual screening of potential compounds

To evaluate the hit compounds obtained from DrugBank and calculate their interaction and binding posture in the active site of target proteins, the molecular docking method was carried out through QuickVina 2 (version 2.1)(*54*). QuickVina 2 is a molecular docking tool developed from the AutoDock Vina(*53*). This shape-based screening method uses the calculation of shape and electrostatic potential similarity of binding pockets to select molecules, which may exhibit binding patterns like those of binding pockets.

3D files of target proteins were dehydrated, hydrogenated. Then CIRP was saved as PDBQT files using AutoDock (*55*). AutoDock assisted in assigning Gasteiger charges and adding polar hydrogen atoms to both the proteins and the compounds.

Molecular dynamics simulation

The molecular dynamics (MD) simulation was performed by Gromacs(*56*). Firstly, a protein-drug complex was prepared, including adding hydrogenation and balancing charge. Then, we add a solvent so that the target protein and drug small molecules are coated. The forcefield was Chemistry at HARvard Macromolecular Mechanics 36 (CHARMm 36). For our weak computing power, the simulation time is set as 50ns. The simulation temperature is 309.15K (36□) and the pressure is 1 atm. Root mean square deviation (RMSD) and root mean square fluctuation (RMSF) of simulations

were calculated based on the first frame.

Personalization-nstart-weight-PageRank

We use personalization-nstart-weight-PageRank to rank all the data of binding scores between drugs and proteins. PageRank is a comprehensive rank algorithm designed by Google and named after Larry Page, Google's co-founder.(*57*) The principle of PageRank is the Markova process over all nodes. PageRank has been applied in multiple medical domains with success.(*58–60*) In this article, the binding of the protein to the drug depends only on the present state, not the past. So, the calculation in this paper satisfied the conditions of the Markov property, and we can use PageRank. The higher the mRNA expression level is, the more important it is through the Markov process.

Personalization, nstart, and weight represent 3 different levels of score data. The weight of PageRank allows all nodes to be initially assigned different weights/probabilities, which can calculate the scores of different nodes more accurately.(*61*) In this article, the weight of rank is set to docking values of proteins and drugs. The higher the docking value, the higher the connection rate of the complex.

Personalization of PageRank reinforces the connection intensity between the nodes, which makes the result more personalized and realistic(*62*). In this article, personalization corresponds to fold changes of proteins, which reflects the importance of the target. Personalization is also influenced by protein functions. If the protein

performs a negative influence such as promoting apoptosis, the personalization will be calculated by 2^(fold change) to make sure all the values are more than 1. Meanwhile, if the protein plays a positive role in the group, the personalization will be set as 1/(fold change + 1) to ensure its value is less than 1. The personalization values of all the drugs are set to 0 to prevent iterations of the drugs themselves from going wrong. Besides, the nstart of PageRank is set to the value of mRNA expression detected by bioinformatics. This indicates the initial amounts of proteins from the beginning of the simulation. The nstarts of drugs are all 0, which means there is no binding of proteins and drugs at the beginning of the simulation.

The calculation process is similar to putting a sufficient amount of all proteins and all drugs in the same solution, then simulating the connections between all proteins and drugs by calculation, and finally comprehensively analyzing the weight of drugs by calculating the number of connections. The damping factor is set to 0.85 to simulate the metabolism of proteins and drugs.

The whole calculation is based on Python 3.8.10. The relating python libraries used in this article include NetworkX, Pandas, and NumPy. We use Pandas and NumPy to import all the docking data into a matrix for PageRank calculating. The protein expression value is then imported by the PageRank personalization parameter of NetworkX. Lastly, we can get a comprehensive ranking of drugs.

Prediction and Rank of combined pharmacotherapy

In addition to the comprehensive ranking of drugs, we also try to generate the rank of drug combinations. Similarly, the calculation places all drugs of combination and

target proteins in a solution to bind free. The specific process is as follows.

First, all drugs should be grouped according to the number of drugs in each combination. In this article, to reduce the amount of calculation, we selected the drugs with the highest ranking of each protein to include in the drug combination pool. Then, all the combinations were performed personalization weight PageRank against all protein targets. The sum of each score of all drugs in the combination is the final score of the combination. Lastly, we get the rank of combinations.

However, the rank obtained by such calculation has a certain defect. The scores obtained by computer simulation do not directly correspond to the probability of protein-molecule binding. There is a mapping function between them. Most mapping functions are set to monotonically increase, and they change by different simulation types and protein structures. This difference produces less error at the top and bottom of the rankings after the Markov process. But for drugs in the middle are highly uncertain. This problem has less impact on the comprehensive drug ranking. However, when the calculation is applied to the drug combination, it reduces the value of ranking. To alleviate the problem, we propose drug-protein-expression fit score (DPEFS) to show the data distribution pattern.

The calculation is as follows:

$$DPEFS = \left(\sum_{i=1}^{n} PR_{(drug)i}\right) \cdot \left(\sum_{t=1}^{m} PR_{(target)t} \cdot E_{(target)t}\right) \Big/ PR_{(target)1}$$

PR is the result of PageRank. E means the logFC of targets. $PR_{(target)1}$ is the first target. It is used for standardized calculation for comparing different combinations.

DPEFS evaluates the combination by referring to the protein expression trend. The higher the DPEFS, the better the fitness. In actual drug design, DPEFS is relatively high and PageRank score is relatively low, indicating that drugs of combination are

relatively moderate, which suggests a negative outcome. All code can be found in GitHub (https://github.com/FeiLiuEM/PageRank-weight-drug).

Result

Expression analysis and clustering of hypothermia

Figure 2 shows the expression of different mRNA of different groups after mild hypothermia. From the inside to the outside, the rings were divided into hypothermia 0.5h group, hypothermia 1H group, hypothermia 2H group, hypothermia 3H group, hypothermia 8h group, and hypothermia 18h group. Among all the mRNA, CIRP showed the highest expression level in mild hypothermia. The expression of CIRP gradually increased after mild hypothermia and reached the highest level after 18 hours of hypothermia.

As shown in Table 1, in each group, we selected the top 3 expression protein targets. In the Hypothermia 0.5h group, the target proteins are circadian-associated transcriptional repressor (CIART), Glutathione-specific gamma-glutamylcyclotransferase 1 (CHAC1), and Uridine diphosphate glucose pyrophosphatase nudix hydrolase 22 (NUDT22). The target proteins of the Hypothermia 1h group are CHAC1, corneodesmosin (CDSN), and Nuclear receptor subfamily 1 group D member 1 (NR1D1). The target proteins of the Hypothermia 2h group are cold-induced RNA-binding protein (CIRP), armadillo repeat-containing X-linked protein 5 (ARMCX5), and coiled-coil domain-containing protein 122 (CCDC122). The target proteins of the Hypothermia 4h group are CIRP, receptor activity-modifying protein 3 (RAMP3), and carcinoembryonic antigen-related cell adhesion molecule 1 (CEACAM1). The target proteins of the Hypothermia 4h group are the same: CIRP, RAMP3, and NAD(P)H dehydrogenase [quinone] 1 (NQO1). Within the targets, CHAC1 could enhance apoptosis(*63*). NUDT22 is a Mg^{2+}-dependent UDP-glucose and UDP-galactose hydrolase(*64*), while high glucose shows a negative effect in HIE like stroke(*65*). CCDC122 potentially pro-inflammatory(*66*).

CIRP can effectively reduce cell death in the early stage of hypothermia therapy. However, it has a strong pro-inflammatory effect outside the cell, leading to cell killing. There is no definitive research on the timing of this shift. Referring to the previous article(*67*), we conservatively believed that CIRP could be identified as negative protein from 8H group. CEACAM1(*68*) and NQO1(*69*) promote apoptosis. All the other targets are shown protective effects or don't have enough data. The personalization values were calculated and in Table 1.

All the structures of target proteins in Figure 3 were obtained by the rules in the section of Materials and Methods.

Visualize evolutionary conservation and Structure-Function Relationship-Based Binding Site Prediction

The conservation analysis of all the target proteins was listed in Figure 4. The redder the amino acid, the more conserved the amino acid sequence, and the more likely it is to have a function.

Then we identified its structure-function relationship by the COACH-D server. The results showed a familiar result of conservation analysis listed in Figure 4.

Also, cross-validation of the predicted residues at the active region was further supported by the results produced in the Site Finder tool of the MOE suite. As shown in Table 2, the range around 3-5 Å of the active site was used for the setting of the receptor pocket of the target proteins that were used for virtual screening.

Virtual Screening of target proteins' Antagonists

We utilized the virtual screening technique to identify potential antagonists exhibiting an adequate binding a□nity. We started with a chemical database consisting of 8,697

drug molecules and isolated a set of compounds satisfying the threshold of a high docking score. The results of the best match complexes are shown in Figure 5 and all the results are listed in the Additional file Table 1.

MD Simulations and Binding Free Energy Analysis

We performed MD simulation of 11 complexes to measure the stability of the protein-ligand complex. RMSD (root-mean-square deviation) profiles of the protein are shown in Figure 6A, which indicates that all systems were relatively stable during the entire simulation run. Moreover, RMSF (Root Mean Square Fluctuation) profiles of protein are measured to evaluate the moving of each amino acid. The result shows that some amino acids of ARMCX, CCDC122, CEACAM, CIART, and RAMP3 are relatively high. And they are available for further analysis (Figure 6B).

The RMSD of drug atoms was also conducted to predict the stability of the atoms in docked complexes (Figure 6C). Most compounds exhibited a consistently low RMSD, suggesting that these compounds formed stable complexes.

Drug rank of TH in different groups

We rank all drugs by PageRank. First, we PageRank all the drugs and get the results in table3. 2-drug-combinations are ranked in Table 4 and 3-drug-combinations in the additional file Table 2. For comprehensive rank, the results of PageRank were listed. For drug-combination ranks, the percentages of each drug's value in the combination were calculated. And DPEFS was calculated for analyzing the distribution differences of drug combinations.

Discussion

In this paper, a new pharmacological method — bioinfo-pharmacology is proposed, using therapeutic hypothermia as an example. In this method, by bioinformatics analysis, protein structure prediction, and PageRank, we provide a direct bridge between symptom/treatment and drug design.

We first analyzed the significant stage-specific differentially expressed genes of hypothermia treatment based on previously published data(*20*). Then, all the compliant proteins were screened out for each group. Then, all target proteins' structures were predicted by neural networks (AlphaFold2 or RoseTTAFold). Later, we predicted the activate sites of all proteins by COACH-D(*45*, *46*), and screened the drugs based on the 3D structures. Lastly, ranks of single-drug and drug combinations were calculated by PageRank.

AlphaFold2 and RoseTTAFold were used for protein structure prediction. And the number of proteins selected by AlphaFold2 in this research was similar to that of RoseTTAFold. During the process of protein structure prediction, we found that for some proteins, the structure predicted by RoseTTAFold has less region of irregular structure than that of AlphaFold2. This may be due to the 2D distance map level transformed and integrated by RoseTTAFold during neural network training(*10*), while AlphaFold2 paired structure database and genetic database. We also find a phenomenon that the predicted protein structures were relatively unstable under molecular dynamics simulation than preview reports of protein structures detected by X-ray. (*70*)

The application of PageRank is suitable. First, the combination of drug molecules is a

memoryless stochastic process, which meets the qualifications of the Markov process. Second, our method aims to simulate the binding process in *vivo*. The comprehensive analysis involves free docking of proteins with all drugs. Drug combination analysis is to put proteins and related drugs into the solution for docking.

Besides, the method has good compatibility for the wide compatibility of PageRank. In theory, all the technologies with numerical results can be ranked by the method. In this paper, for the lack of bioinformatics data of Therapeutic hypothermia, we only do a basic analysis. If there is more data of the TH, the analysis of Weighted Gene Coexpression Network Analysis (WGCNA)[58] or Gene Regulatory Networks (GRN)(*71*) will be better because they could provide more plausible results of protein list.

For the same reason, this method can also enhance network pharmacology. Network pharmacologye(*12*) focuses on the application of protein network structures to improve drug discovery. By PageRank, the association between protein network structures and different drugs can be more accurately understood through comprehensive drug analysis of multiple targets rather than the previous single target. Another influenced area is chrono-pharmacology. Chrono-pharmacology(*72*) is expert in the adaptation and anticipation mechanisms of the body concerning clock system regulation of various kinetic and dynamic pathways, including absorption, distribution, metabolism, and excretion of drugs and nutrients. By bioinfo-pharmacology, researchers can develop drugs for different time groups.

Besides, pharmacophore models(*73*) can use bioinfo-pharmacology for highly efficient drug design. After analyzing, top-ranked pharmacophore fingerprints or

alignments could be considered to be linked together for good pharmacological effects. And ultimately, improve the therapeutic effect of drugs, reduce toxic and side effects, improve the success rate of clinical trials of new drugs, save drug research and development costs.

Based on these potential improvements and high compatibility, we propose the concept of bioinfo-pharmacology for its ability to directly apply bioinformatics for drug discovery. Bioinfo-pharmacology is a method that uses bioinformatics, protein structure prediction, and PageRank for drug design. The main feature is that multiple targets target multiple molecules/pharmacophores. Overall, this approach builds a bridge between disease/treatment and drug development, bringing up more possibilities for future drug development.

Bioinfo-pharmacology can assist the existing therapeutic techniques. First, the techniques presented in this paper have direct benefits for precision medicine(*74*). This paper can directly analyze the suitable and unsuitable use of hypothermia therapy. The results obtained can guide the appropriate drug and the drug to be avoided in the clinical practice of TH. With rapid drug delivery technologies such as deep venous catheterization, we can more precisely control drug delivery to improve treatment outcomes. Secondly, our research has a good promotion effect on traditional herbal medicine research. In traditional herbal medicine, there may be multiple drug molecules in a single herb, and its complex multi-target problem can be efficiently analyzed by new methods. In addition, rational analysis of drug combinations was also carried out in this paper, which had not appeared before.

In addition, the research brings more possibilities for drug development. The most

recognized current drug development technology is the pharmacophore model. Docking with the target through the pharmacophore, and then expanding against the pharmacophore. Through this paper, we can directly rank the pharmacophore of all targets. Not only that, but a combination of all the pharmacophores could theoretically achieve better results than a single pharmacophore. Theoretically, through the rational combination of pharmacophore, we can directly obtain the optimal drugs corresponding to the group. Our technology may be changing the process of drug discovery.

This research has some defects. 1: For the speed of calculating, we only choose the top 3 mRNAs and use the top 1 complex for MD simulation. Furthermore, the duration of molecular dynamics simulation is set to 50ns. These operations mitigate the rationality of the results relatively; 2. Theoretically, pharmacophore modeling has a better improvement under PageRank. But considering the purpose of the article, we use AutoDock to dock all the marketing drugs.

In summary, this paper proposes a new method of pharmacology—bioinfo-pharmacology by PageRank. The results provide medical clues for the treatment of TH. Besides, it can help the functional research of proteins at the molecular level for experimental biologists. In addition, we can do drug combination analysis of drugs similarly. The new approach could have a huge impact on precision medicine, drug design, and traditional herbal medicine in the future.

Reference

1. J. A. DiMasi, H. G. Grabowski, R. W. Hansen, Innovation in the pharmaceutical industry: New estimates of R&D costs. *J. Health Econ.* **47**, 20–33 (2016).

2. J. Hughes, S. Rees, S. Kalindjian, K. Philpott, Principles of early drug discovery: Principles of early drug discovery. *Br. J. Pharmacol.* **162**, 1239–1249 (2011).

3. F. Ban, K. Dalal, H. Li, E. LeBlanc, P. S. Rennie, A. Cherkasov, Best Practices of Computer-Aided Drug Discovery: Lessons Learned from the Development of a Preclinical Candidate for Prostate Cancer with a New Mechanism of Action. *J. Chem. Inf. Model.* **57**, 1018–1028 (2017).

4. H. Jhoti, S. Rees, R. Solari, High-throughput screening and structure-based approaches to hit discovery: is there a clear winner? *Expert Opin. Drug Discov.* **8**, 1449–1453 (2013).

5. S. J. Y. Macalino, V. Gosu, S. Hong, S. Choi, Role of computer-aided drug design in modern drug discovery. *Arch. Pharm. Res.* **38**, 1686–1701 (2015).

6. R. Li, Y. Li, X. Liang, L. Yang, M. Su, K. P. Lai, Network Pharmacology and bioinformatics analyses identify intersection genes of niacin and COVID-19 as potential therapeutic targets. *Brief. Bioinform*. **22**, 1279–1290 (2021).

7. N. R. Gandasi, P. Yin, M. Omar-Hmeadi, E. Ottosson Laakso, P. Vikman, S. Barg, Glucose-Dependent Granule Docking Limits Insulin Secretion and Is Decreased in Human Type 2 Diabetes. *Cell Metab*. **27**, 470-478.e4 (2018).

8. A. Cypionka, A. Stein, J. M. Hernandez, H. Hippchen, R. Jahn, P. J. Walla, Discrimination between docking and fusion of liposomes reconstituted with neuronal SNARE-proteins using FCS. *Proc. Natl. Acad. Sci. U. S. A.* **106**, 18575–18580 (2009).

9. J. Jumper, R. Evans, A. Pritzel, T. Green, M. Figurnov, O. Ronneberger, K. Tunyasuvunakool, R. Bates, A. Žídek, A. Potapenko, A. Bridgland, C. Meyer, S. A. A. Kohl, A. J. Ballard, A. Cowie, B. Romera-Paredes, S. Nikolov, R. Jain, J. Adler, T. Back, S. Petersen, D. Reiman, E. Clancy, M. Zielinski, M. Steinegger, M. Pacholska, T. Berghammer, S. Bodenstein, D. Silver, O. Vinyals, A. W. Senior, K. Kavukcuoglu, P. Kohli, D. Hassabis, Highly accurate protein structure prediction with AlphaFold. *Nature*. **596**, 583–589 (2021).

10. M. Baek, F. DiMaio, I. Anishchenko, J. Dauparas, S. Ovchinnikov, G. R. Lee, J. Wang, Q. Cong, L. N. Kinch, R. D. Schaeffer, C. Millán, H. Park, C. Adams, C. R. Glassman, A. DeGiovanni, J. H. Pereira, A. V. Rodrigues, A. A. van Dijk, A. C. Ebrecht, D. J. Opperman, T. Sagmeister, C. Buhlheller, T. Pavkov-Keller, M. K. Rathinaswamy, U. Dalwadi, C. K. Yip, J. E. Burke, K. C. Garcia, N. V. Grishin, P. D. Adams, R. J. Read, D. Baker, Accurate prediction of protein structures and interactions using a three-track neural network. *Science*. **373**, 871–876 (2021).

11. E. Solano-Gonzalez, K. M. Coburn, W. Yu, G. M. Wilson, E. Nurmemmedov, S. Kesari, E. T. Chang, A. D. MacKerell, D. J. Weber, F. Carrier, Small molecules inhibitors of the heterogeneous ribonuclear protein A18 (hnRNP A18): a regulator of protein translation and an immune checkpoint. *Nucleic Acids Res.* **49**, 1235–1246 (2021).

12. A. L. Hopkins, Network pharmacology: the next paradigm in drug discovery. *Nat. Chem. Biol.* **4**, 682–690 (2008).

13. S. K. Wooller, G. Benstead-Hume, X. Chen, Y. Ali, F. M. G. Pearl, Bioinformatics in translational drug discovery. *Biosci. Rep.* **37**, BSR20160180 (2017).

14. J.-B. Lascarrou, H. Merdji, A. Le Gouge, G. Colin, G. Grillet, P. Girardie, E. Coupez, P.-F. Dequin, A. Cariou, T. Boulain, N. Brule, J.-P. Frat, P. Asfar, N. Pichon, M. Landais, G. Plantefeve, J.-P. Quenot, J.-C. Chakarian, M. Sirodot, S. Legriel, J. Letheulle, D. Thevenin, A. Desachy, A. Delahaye, V. Botoc, S. Vimeux, F. Martino, B. Giraudeau, J. Reignier, CRICS-TRIGGERSEP Group, Targeted Temperature Management for Cardiac Arrest with Nonshockable Rhythm. *N. Engl. J. Med*. **381**, 2327–2337 (2019).

15. J. Y. Kim, J. H. Kim, J. Park, J. H. Beom, S. P. Chung, J. S. You, J. E. Lee, Targeted Temperature Management at 36 °C Shows Therapeutic Effectiveness via Alteration of Microglial Activation and Polarization After Ischemic Stroke. *Transl. Stroke Res.* (2021), doi:10.1007/s12975-021-00910-8.

16. M. Hosseini, R. H. Wilson, C. Crouzet, A. Amirhekmat, K. S. Wei, Y. Akbari, Resuscitating the Globally Ischemic Brain: TTM and Beyond. *Neurother. J. Am. Soc. Exp. Neurother.* **17**, 539–562 (2020).

17. M. F. Hazinski, J. P. Nolan, R. Aickin, F. Bhanji, J. E. Billi, C. W. Callaway, M. Castren, A. R. de Caen, J. M. E. Ferrer, J. C. Finn, L. M. Gent, R. E. Griffin, S. Iverson, E. Lang, S. H. Lim, I. K. Maconochie, W. H. Montgomery, P. T. Morley, V. M. Nadkarni, R. W. Neumar, N. I. Nikolaou, G. D. Perkins, J. M. Perlman, E. M. Singletary, J. Soar, A. H. Travers, M. Welsford, J. Wyllie, D. A. Zideman, Part 1: Executive Summary: 2015 International Consensus on Cardiopulmonary Resuscitation and Emergency Cardiovascular Care Science With Treatment Recommendations. *Circulation*. **132**, S2-39 (2015).

18. V. Lemiale, F. Dumas, N. Mongardon, O. Giovanetti, J. Charpentier, J.-D. Chiche, P. Carli, J.-P. Mira, J. Nolan, A. Cariou, Intensive care unit mortality after cardiac arrest: the relative contribution of shock and brain injury in a large cohort. *Intensive Care Med.* **39**, 1972–1980 (2013).

19. L.-M. Rosenthal, C. Leithner, G. Tong, K. J. Streitberger, J. Krech, C. Storm, K. R. L. Schmitt, RBM3 and CIRP expressions in targeted temperature management treated cardiac arrest patients-A prospective single center study. *PloS One*. **14**, e0226005 (2019).

20. S. Ilmjärv, C. A. Hundahl, R. Reimets, M. Niitsoo, R. Kolde, J. Vilo, E. Vasar, H. Luuk, Estimating differential expression from multiple indicators. *Nucleic Acids Res.* **42**, e72 (2014).

21. A. Artero-Castro, F. B. Callejas, J. Castellvi, H. Kondoh, A. Carnero, P. J. Fernández-Marcos, M. Serrano, S. Ramón y Cajal, M. E. Lleonart, Cold-inducible RNA-binding protein bypasses replicative senescence in primary cells through extracellular signal-regulated kinase 1 and 2 activation. *Mol. Cell. Biol.* **29**, 1855–1868 (2009).

22. R. Yang, M. Zhan, N. R. Nalabothula, Q. Yang, F. E. Indig, F. Carrier, Functional significance for a heterogenous ribonucleoprotein A18 signature RNA motif in the 3'-untranslated region of ataxia telangiectasia mutated and Rad3-related (ATR) transcript. *J. Biol. Chem*. **285**, 8887–8893 (2010).

23. B. Haley, T. Paunesku, M. Protić, G. E. Woloschak, Response of heterogeneous ribonuclear proteins (hnRNP) to ionising radiation and their involvement in DNA damage repair. *Int. J. Radiat. Biol.* **85**, 643–655 (2009).

24. R. Yang, D. J. Weber, F. Carrier, Post-transcriptional regulation of thioredoxin by the stress inducible heterogenous ribonucleoprotein A18. *Nucleic Acids Res.* **34**, 1224–1236 (2006).

25. Y. Peng, P.-H. Yang, J. A. Tanner, J.-D. Huang, M. Li, H. F. Lee, R.-H. Xu, H.-F. Kung, M. C. M. Lin, Cold-inducible RNA binding protein is required for the expression of adhesion molecules and embryonic cell movement in Xenopus laevis. *Biochem. Biophys. Res.*

Commun. **344**, 416–424 (2006).

26. J. Morf, G. Rey, K. Schneider, M. Stratmann, J. Fujita, F. Naef, U. Schibler, Cold-inducible RNA-binding protein modulates circadian gene expression posttranscriptionally. *Science*. **338**, 379–383 (2012).

27. Z. Xia, X. Zheng, H. Zheng, X. Liu, Z. Yang, X. Wang, Cold-inducible RNA-binding protein (CIRP) regulates target mRNA stabilization in the mouse testis. *FEBS Lett.* **586**, 3299–3308 (2012).

28. Y. Zhang, Y. Wu, P. Mao, F. Li, X. Han, Y. Zhang, S. Jiang, Y. Chen, J. Huang, D. Liu, Y. Zhao, W. Ma, Z. Songyang, Cold-inducible RNA-binding protein CIRP/hnRNP A18 regulates telomerase activity in a temperature-dependent manner. *Nucleic Acids Res.* **44**, 761–775 (2016).

29. P. Zhong, H. Huang, Recent progress in the research of cold-inducible RNA-binding protein. *Future Sci. OA*. **3**, FSO246 (2017).

30. T. Sakurai, H. Kashida, T. Watanabe, S. Hagiwara, T. Mizushima, H. Iijima, N. Nishida, H. Higashitsuji, J. Fujita, M. Kudo, Stress response protein cirp links inflammation and tumorigenesis in colitis-associated cancer. *Cancer Res.* **74**, 6119–6128 (2014).

31. T. Sakurai, H. Kashida, Y. Komeda, T. Nagai, S. Hagiwara, T. Watanabe, M. Kitano, N. Nishida, J. Fujita, M. Kudo, Stress Response Protein RBM3 Promotes the Development of Colitis-associated Cancer. *Inflamm. Bowel Dis.* **23**, 57–65 (2017).

32. F.-C. Gong, R. Ji, Y.-M. Wang, Z.-T. Yang, Y. Chen, E.-Q. Mao, E.-Z. Chen, Identification of Potential Biomarkers and Immune Features of Sepsis Using Bioinformatics Analysis. *Mediators Inflamm.* **2020**, 3432587 (2020).

33. T. Galili, dendextend: an R package for visualizing, adjusting and comparing trees of hierarchical clustering. *Bioinforma. Oxf. Engl.* **31**, 3718–3720 (2015).

34. S. Kothakota, T. Azuma, C. Reinhard, A. Klippel, J. Tang, K. Chu, T. J. McGarry, M. W. Kirschner, K. Koths, D. J. Kwiatkowski, L. T. Williams, Caspase-3-generated fragment of gelsolin: effector of morphological change in apoptosis. *Science*. **278**, 294–298 (1997).

35. J. Jumper, R. Evans, A. Pritzel, T. Green, M. Figurnov, O. Ronneberger, K. Tunyasuvunakool, R. Bates, A. Žídek, A. Potapenko, A. Bridgland, C. Meyer, S. A. A. Kohl, A. J. Ballard, A. Cowie, B. Romera-Paredes, S. Nikolov, R. Jain, J. Adler, T. Back, S. Petersen, D. Reiman, E. Clancy, M. Zielinski, M. Steinegger, M. Pacholska, T. Berghammer, D. Silver, O. Vinyals, A. W. Senior, K. Kavukcuoglu, P. Kohli, D. Hassabis, Applying and improving AlphaFold at CASP14. *Proteins* (2021), doi:10.1002/prot.26257.

36. H. Bagdonas, C. A. Fogarty, E. Fadda, J. Agirre, The case for post-predictional modifications in the AlphaFold Protein Structure Database. *Nat. Struct. Mol. Biol.* **28**, 869–870 (2021).

37. J. K. Leman, B. D. Weitzner, S. M. Lewis, J. Adolf-Bryfogle, N. Alam, R. F. Alford, M. Aprahamian, D. Baker, K. A. Barlow, P. Barth, B. Basanta, B. J. Bender, K. Blacklock, J. Bonet, S. E. Boyken, P. Bradley, C. Bystroff, P. Conway, S. Cooper, B. E. Correia, B. Coventry, R. Das, R. M. De Jong, F. DiMaio, L. Dsilva, R. Dunbrack, A. S. Ford, B. Frenz, D. Y. Fu, C. Geniesse, L. Goldschmidt, R. Gowthaman, J. J. Gray, D. Gront, S. Guffy, S. Horowitz, P.-S. Huang, T. Huber, T. M. Jacobs, J. R. Jeliazkov, D. K. Johnson, K. Kappel, J. Karanicolas, H. Khakzad, K. R. Khar, S. D. Khare, F. Khatib, A. Khramushin, I. C. King, R. Kleffner, B. Koepnick, T. Kortemme, G. Kuenze, B. Kuhlman, D. Kuroda, J. W. Labonte, J. K. Lai, G. Lapidoth, A. Leaver-Fay, S. Lindert, T. Linsky, N. London, J. H. Lubin, S. Lyskov,

J. Maguire, L. Malmström, E. Marcos, O. Marcu, N. A. Marze, J. Meiler, R. Moretti, V. K. Mulligan, S. Nerli, C. Norn, S. Ó'Conchúir, N. Ollikainen, S. Ovchinnikov, M. S. Pacella, X. Pan, H. Park, R. E. Pavlovicz, M. Pethe, B. G. Pierce, K. B. Pilla, B. Raveh, P. D. Renfrew, S. S. R. Burman, A. Rubenstein, M. F. Sauer, A. Scheck, W. Schief, O. Schueler-Furman, Y. Sedan, A. M. Sevy, N. G. Sgourakis, L. Shi, J. B. Siegel, D.-A. Silva, S. Smith, Y. Song, A. Stein, M. Szegedy, F. D. Teets, S. B. Thyme, R. Y.-R. Wang, A. Watkins, L. Zimmerman, R. Bonneau, Macromolecular modeling and design in Rosetta: recent methods and frameworks. *Nat. Methods*. **17**, 665–680 (2020).

38. I. R. Humphreys, J. Pei, M. Baek, A. Krishnakumar, I. Anishchenko, S. Ovchinnikov, J. Zhang, T. J. Ness, S. Banjade, S. R. Bagde, V. G. Stancheva, X.-H. Li, K. Liu, Z. Zheng, D. J. Barrero, U. Roy, J. Kuper, I. S. Fernández, B. Szakal, D. Branzei, J. Rizo, C. Kisker, E. C. Greene, S. Biggins, S. Keeney, E. A. Miller, J. C. Fromme, T. L. Hendrickson, Q. Cong, D. Baker, Computed structures of core eukaryotic protein complexes. *Science*, eabm4805 (2021).

39. D. S. Wishart, Y. D. Feunang, A. C. Guo, E. J. Lo, A. Marcu, J. R. Grant, T. Sajed, D. Johnson, C. Li, Z. Sayeeda, N. Assempour, I. Iynkkaran, Y. Liu, A. Maciejewski, N. Gale, A. Wilson, L. Chin, R. Cummings, D. Le, A. Pon, C. Knox, M. Wilson, DrugBank 5.0: a major update to the DrugBank database for 2018. *Nucleic Acids Res.* **46**, D1074–D1082 (2018).

40. H. Ashkenazy, S. Abadi, E. Martz, O. Chay, I. Mayrose, T. Pupko, N. Ben-Tal, ConSurf 2016: an improved methodology to estimate and visualize evolutionary conservation in macromolecules. *Nucleic Acids Res.* **44**, W344-350 (2016).

41. A. Biegert, J. Söding, Sequence context-specific profiles for homology searching. *Proc. Natl. Acad. Sci. U. S. A.* **106**, 3770–3775 (2009).

42. B. E. Suzek, Y. Wang, H. Huang, P. B. McGarvey, C. H. Wu, UniProt Consortium, UniRef clusters: a comprehensive and scalable alternative for improving sequence similarity searches. *Bioinforma. Oxf. Engl.* **31**, 926–932 (2015).

43. K. Katoh, D. M. Standley, MAFFT multiple sequence alignment software version 7: improvements in performance and usability. *Mol. Biol. Evol.* **30**, 772–780 (2013).

44. T. Pupko, R. E. Bell, I. Mayrose, F. Glaser, N. Ben-Tal, Rate4Site: an algorithmic tool for the identification of functional regions in proteins by surface mapping of evolutionary determinants within their homologues. *Bioinforma. Oxf. Engl.* **18 Suppl 1**, S71-77 (2002).

45. J. Yang, A. Roy, Y. Zhang, Protein-ligand binding site recognition using complementary binding-specific substructure comparison and sequence profile alignment. *Bioinforma. Oxf. Engl.* **29**, 2588–2595 (2013).

46. Q. Wu, Z. Peng, Y. Zhang, J. Yang, COACH-D: improved protein-ligand binding sites prediction with refined ligand-binding poses through molecular docking. *Nucleic Acids Res.* **46**, W438–W442 (2018).

47. J. Yang, R. Yan, A. Roy, D. Xu, J. Poisson, Y. Zhang, The I-TASSER Suite: protein structure and function prediction. *Nat. Methods.* **12**, 7–8 (2015).

48. A. Roy, J. Yang, Y. Zhang, COFACTOR: an accurate comparative algorithm for structure-based protein function annotation. *Nucleic Acids Res.* **40**, W471-477 (2012).

49. M. Brylinski, J. Skolnick, A threading-based method (FINDSITE) for ligand-binding site prediction and functional annotation. *Proc. Natl. Acad. Sci. U. S. A.* **105**, 129–134 (2008).

50. J. Yang, A. Roy, Y. Zhang, BioLiP: a semi-manually curated database for biologically

relevant ligand-protein interactions. *Nucleic Acids Res.* **41**, D1096-1103 (2013).

51. P. W. Rose, A. Prlić, A. Altunkaya, C. Bi, A. R. Bradley, C. H. Christie, L. D. Costanzo, J. M. Duarte, S. Dutta, Z. Feng, R. K. Green, D. S. Goodsell, B. Hudson, T. Kalro, R. Lowe, E. Peisach, C. Randle, A. S. Rose, C. Shao, Y.-P. Tao, Y. Valasatava, M. Voigt, J. D. Westbrook, J. Woo, H. Yang, J. Y. Young, C. Zardecki, H. M. Berman, S. K. Burley, The RCSB protein data bank: integrative view of protein, gene and 3D structural information. *Nucleic Acids Res.* **45**, D271–D281 (2017).

52. J. A. Capra, R. A. Laskowski, J. M. Thornton, M. Singh, T. A. Funkhouser, Predicting protein ligand binding sites by combining evolutionary sequence conservation and 3D structure. *PLoS Comput. Biol.* **5**, e1000585 (2009).

53. O. Trott, A. J. Olson, AutoDock Vina: improving the speed and accuracy of docking with a new scoring function, efficient optimization, and multithreading. *J. Comput. Chem.* **31**, 455–461 (2010).

54. A. Alhossary, S. D. Handoko, Y. Mu, C.-K. Kwoh, Fast, accurate, and reliable molecular docking with QuickVina 2. *Bioinforma. Oxf. Engl.* **31**, 2214–2216 (2015).

55. G. M. Morris, R. Huey, W. Lindstrom, M. F. Sanner, R. K. Belew, D. S. Goodsell, A. J. Olson, AutoDock4 and AutoDockTools4: Automated docking with selective receptor flexibility. *J. Comput. Chem.* **30**, 2785–2791 (2009).

56. D. Van Der Spoel, E. Lindahl, B. Hess, G. Groenhof, A. E. Mark, H. J. C. Berendsen, GROMACS: fast, flexible, and free. *J. Comput. Chem.* **26**, 1701–1718 (2005).

57. L. Page, S. Brin, R. Motwani, T. Winograd, “The PageRank Citation Ranking: Bringing Order to the Web.” (Technical Report 1999–66, Stanford InfoLab, 1999), (available at http://ilpubs.stanford.edu:8090/422/).

58. A. Halu, R. J. Mondragón, P. Panzarasa, G. Bianconi, Multiplex PageRank. *PloS One*. **8**, e78293 (2013).

59. K. Kalecky, Y.-R. Cho, PrimAlign: PageRank-inspired Markovian alignment for large biological networks. *Bioinforma. Oxf. Engl.* **34**, i537–i546 (2018).

60. L. Chen, L. Heikkinen, C. Wang, Y. Yang, H. Sun, G. Wong, Trends in the development of miRNA bioinformatics tools. *Brief. Bioinform.* **20**, 1836–1852 (2019).

61. W. Xing, A. Ghorbani, in *Proceedings. Second Annual Conference on Communication Networks and Services Research, 2004.* (2004), pp. 305–314.

62. T. Haveliwala, S. Kamvar, G. Jeh, “An Analytical Comparison of Approaches to Personalizing PageRank” (Technical Report 2003–35, Stanford, 2003), (available at http://ilpubs.stanford.edu:8090/596/).

63. I. N. Mungrue, J. Pagnon, O. Kohannim, P. S. Gargalovic, A. J. Lusis, CHAC1/MGC4504 is a novel proapoptotic component of the unfolded protein response, downstream of the ATF4-ATF3-CHOP cascade. *J. Immunol. Baltim. Md 1950*. **182**, 466–476 (2009).

64. M. Carter, A.-S. Jemth, J. Carreras-Puigvert, P. Herr, M. Martínez Carranza, K. S. A. Vallin, A. Throup, T. Helleday, P. Stenmark, Human NUDT22 Is a UDP-Glucose/Galactose Hydrolase Exhibiting a Unique Structural Fold. *Struct. Lond. Engl. 1993*. **26**, 295-303.e6 (2018).

65. S. Zhang, W. Zuo, X.-F. Guo, W.-B. He, N.-H. Chen, Cerebral glucose transporter: the

possible therapeutic target for ischemic stroke. *Neurochem. Int.* **70**, 22–29 (2014).

66. A. L. Leturiondo, A. B. Noronha, C. Y. R. Mendonça, C. de O. Ferreira, L. E. Alvarado-Arnez, F. S. de N. Manta, O. C. de L. Bezerra, E. F. de Carvalho, M. O. Moraes, F. da C. Rodrigues, C. Talhari, Association of NOD2 and IFNG single nucleotide polymorphisms with leprosy in the Amazon ethnic admixed population. *PLoS Negl. Trop. Dis.* **14**, e0008247 (2020).

67. N.-L. Denning, W.-L. Yang, L. Hansen, J. Prince, P. Wang, C23, an oligopeptide derived from cold-inducible RNA-binding protein, suppresses inflammation and reduces lung injury in neonatal sepsis. *J. Pediatr. Surg.* **54**, 2053–2060 (2019).

68. C. Zhao, Z. Dang, J. Sun, S. Yuan, L. Xie, Up-regulation of microRNA-30b/30d cluster represses hepatocyte apoptosis in mice with fulminant hepatic failure by inhibiting CEACAM1. *IUBMB Life*. **72**, 1349–1363 (2020).

69. Y. Feng, R. Cui, Z. Li, X. Zhang, Y. Jia, X. Zhang, J. Shi, K. Qu, C. Liu, J. Zhang, Methane Alleviates Acetaminophen-Induced Liver Injury by Inhibiting Inflammation, Oxidative Stress, Endoplasmic Reticulum Stress, and Apoptosis through the Nrf2/HO-1/NQO1 Signaling Pathway. *Oxid. Med. Cell. Longev.* **2019**, 7067619 (2019).

70. Y. Wang, X. Wang, Y. Xiong, C.-D. Li, Q. Xu, L. Shen, A. Chandra Kaushik, D.-Q. Wei, An Integrated Pan-Cancer Analysis and Structure-Based Virtual Screening of GPR15. *Int. J. Mol. Sci.* **20**, E6226 (2019).

71. A. Alexiou, S. Chatzichronis, A. Perveen, A. Hafeez, G. M. Ashraf, Algorithmic and Stochastic Representations of Gene Regulatory Networks and Protein-Protein Interactions. *Curr. Top. Med. Chem.* **19**, 413–425 (2019).

72. Y. Tahara, S. Shibata, Chrono-biology, chrono-pharmacology, and chrono-nutrition. *J. Pharmacol. Sci.* **124**, 320–335 (2014).

73. G. Sliwoski, S. Kothiwale, J. Meiler, E. W. Lowe, Computational methods in drug discovery. *Pharmacol. Rev.* **66**, 334–395 (2014).

74. I. R. König, O. Fuchs, G. Hansen, E. von Mutius, M. V. Kopp, What is precision medicine? *Eur. Respir. J.* **50**, 1700391 (2017).

Table 1. The target proteins of different groups.

Group	Target	logFC	Personalization	Expression/nstart
0.5h	CIART	0.46	0.42	8.02
	CHAC1	0.43	1.34	9.64
	NUDT22	0.40	1.32	9.40
1h	CDSN	0.52	0.41	8.17
	NR1D1	0.50	0.41	10.66
	CHAC1	0.50	1.41	9.71
2h	CIRP	0.80	0.36	9.43
	ARMCX5	0.66	0.39	5.97
	CCDC122	0.49	1.41	8.06
4h	CIRP	1.17	0.31	9.80
	RAMP3	0.91	0.35	9.05
	CEACAM1	0.87	1.82	7.11
8h	CIRP	1.57	2.97	10.20
	RAMP3	1.33	0.28	9.47
	NQO1	1.18	2.27	10.87
18h	CIRP	1.71	3.27	10.34
	NQO1	1.55	2.93	11.25
	RAMP3	1.32	0.29	9.46

Table 2. The docking parameters of target proteins.

Protein name	protein source	X	Y	Z	LEN-X	LEN-Y	LEN-Z
ARMCX5	RoseTTAFold	-7.06	31.20	-43.05	29.25	28.50	24.75
CDSN	RoseTTAFold	51.80	53.51	31.17	39.75	20.25	21.00
CEACAM1	AlphaFold2	-41.13	3.42	5.67	39.75	22.50	22.50
CHAC1	AlphaFold2	-3.04	-0.53	0.22	23.25	25.50	35.25
CIART	RoseTTAFold	36.79	-16.59	-36.23	28.50	38.25	22.50
CIRP	RoseTTAFold	14.48	2.86	-9.56	17.25	15.00	19.50
NQO1	AlphaFold2	-1.86	-16.32	-9.20	29.25	29.25	28.50
NR1D1	RoseTTAFold	0.34	35.70	10.28	39.75	25.50	24.75
NUDT22	AlphaFold2	10.08	-12.04	14.09	17.25	38.25	22.50
RAMP3	AlphaFold2	0.00	-10.93	-5.29	24.00	24.00	21.00
CCDC122	RoseTTAFold	119.27	23.34	8.09	36.00	47.25	47.25

Table 3. The comprehensive rank of drugs at different groups.

Group	**Drug**	**weighted_personalized_PageRank (*10^{-4})**
h0.5h	Fluzoparib	0.81
	Lorecivivint	0.80
	Vactosertib	0.80
h1h	Lorecivivint	0.81
	AC-430	0.81
	Raltegravir	0.80
h2h	Phthalocyanine	0.90
	Vazegepant	0.87
	Bemcentinib	0.86
h4h	Phthalocyanine	0.85
	3-(2-AMINOQUINAZOLIN-6-YL)-4-METHYL-N-[3-(TRIFLUOROMETHYL)PHENYL]BENZAMIDE	0.84
	Bemcentinib	0.84
h8h	Phthalocyanine	0.87
	MK-3207	0.86
	Lifirafenib	0.85
h18h	Phthalocyanine	0.87
	MK-3207	0.86
	Lifirafenib	0.85

Table 4. Rank of 2 drug combinations of different group.

	drug1	drug2	PageRank value of drug1	persent age	PageRank value of drug2	persent age	personalized_weight_PageRank	Drug-protein-expression fit score
h0.5h	Lorecivivint	Fluzoparib	0.41	49.85	0.42	50.15	0.83	2.30
	Vactosertib	Fluzoparib	0.41	49.56	0.42	50.44	0.83	2.33
	2'-deoxy-N-(naphthalen-1-ylmethyl)guanosine 5'-(dihydrogen phosphate)	Fluzoparib	0.41	49.68	0.42	50.32	0.83	2.32
h1h	Lorecivivint	AC-430	0.41	49.67	0.42	50.33	0.83	4.36
	Lorecivivint	Raltegravir	0.42	50.12	0.41	49.88	0.83	4.40
	Lorecivivint	Vactosertib	0.42	50.21	0.41	49.79	0.83	4.37
h2h	Phthalocyanine	Vazegepant	0.42	51.42	0.40	48.58	0.82	4.65
	Phthalocyanine	Bemcentinib	0.43	51.84	0.40	48.16	0.82	4.71
	Phthalocyanine	Lifirafenib	0.43	52.28	0.39	47.72	0.82	4.64
h4h	3-(2-AMINOQUINAZOLIN-6-YL)-4-METHYL-N-[3-(TRIFLUOROMETHYL)PHENYL] BENZAMIDE	CD564	0.41	50.25	0.41	49.75	0.82	1.60

	Adapalene	3-(2-AMINOQUINAZOLIN-6-YL)-4-METHYL-N-[3-(TRIFLUOROMETHYL)PHENYL] BENZAMIDE	0.41	49.90	0.41	50.10	0.82	1.60
	3-(2-AMINOQUINAZOLIN-6-YL)-4-METHYL-N-[3-(TRIFLUOROMETHYL)PHENYL] BENZAMIDE	Phthalocyanine	0.42	50.52	0.41	49.48	0.82	1.60
h8h	Phthalocyanine	MK-3207	0.41	49.91	0.41	50.09	0.83	3.94
	Phthalocyanine	Lifirafenib	0.42	50.17	0.41	49.83	0.83	3.93
	Lifirafenib	MK-3207	0.41	49.75	0.42	50.25	0.83	3.94
h18h	Phthalocyanine	MK-3207	0.41	49.91	0.41	50.09	0.83	4.95
	Lifirafenib	MK-3207	0.41	49.77	0.42	50.23	0.83	4.95
	Phthalocyanine	Lifirafenib	0.42	50.14	0.41	49.86	0.83	4.94

Figure 1. Representative workflow for bioinfo-pharmacology drug design.

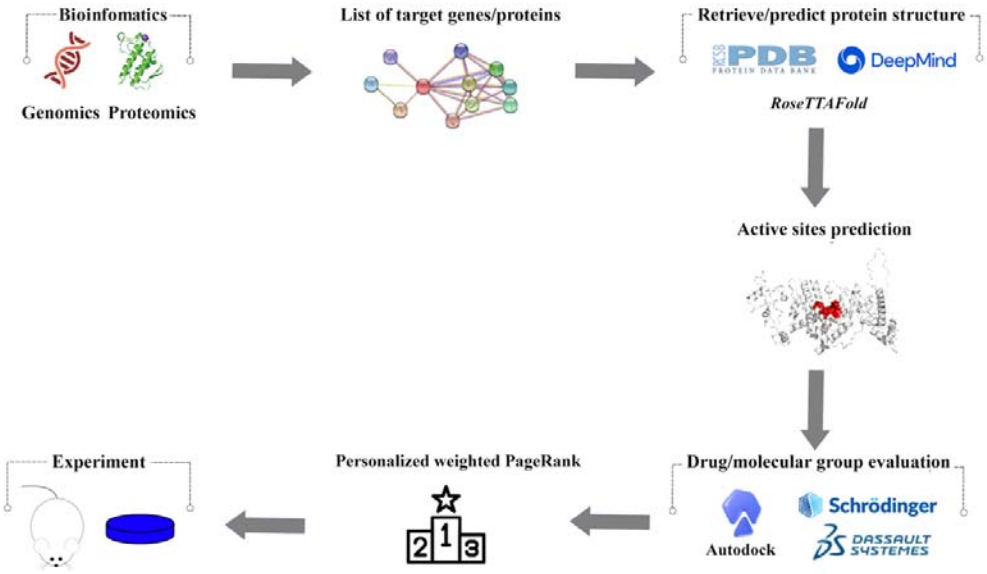

Figure 2. Circular visualization of expression patterns and clustering of hypothermia treatment. Red indicates gene upregulation and blue indicates downregulation.

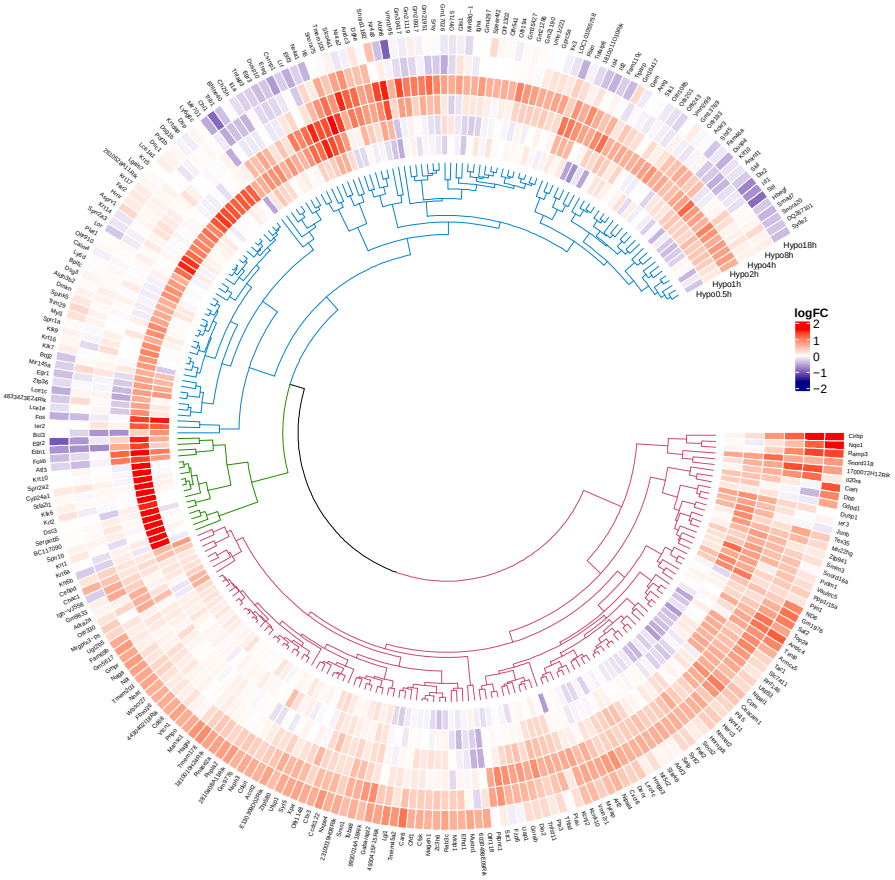

Figure 3. The 3D structures of target proteins. A. ARMCX5; B. CCDC; C. CDSN; D. CEACAM1; E. CHAC1; F. CIART; G. CIRP; H. NQO1; I. NR1D1; J. NUDT22; K. RAMP3.

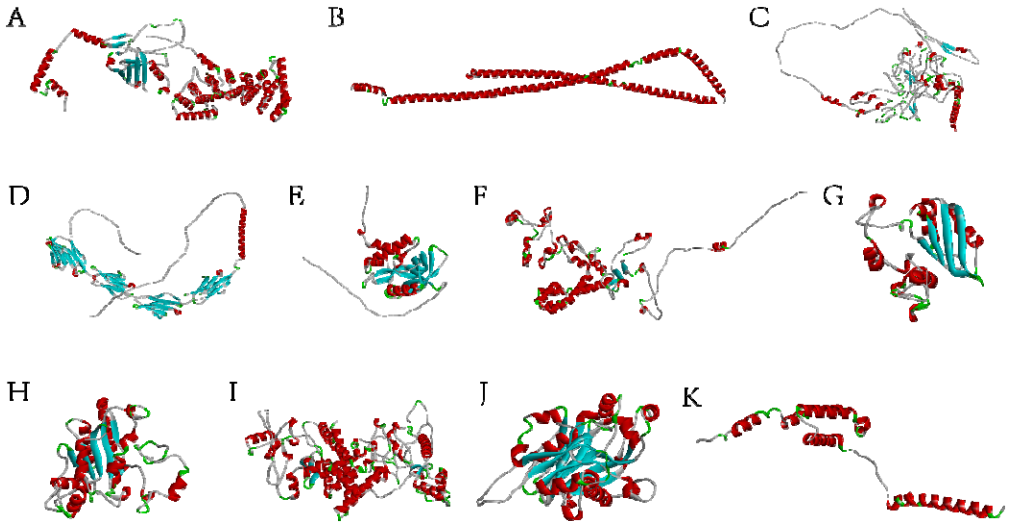

Figure 4. The ConSurf analysis and predicted active sites of target proteins. The upper 11 pictures are ConSurf analysis results. The last 11 pictures are predicted active sites. A&L. ARMCX5; B&M. CCDC; C&N. CDSN; D&O. CEACAM1; E&P. CHAC1; F&Q. CIART; G&R. CIRP; H&S. NQO1; I&T. NR1D1; J&U. NUDT22; K&V. RAMP3. The redder the amino acid, the more conservative it is. The greener the color, the less conservative it is.

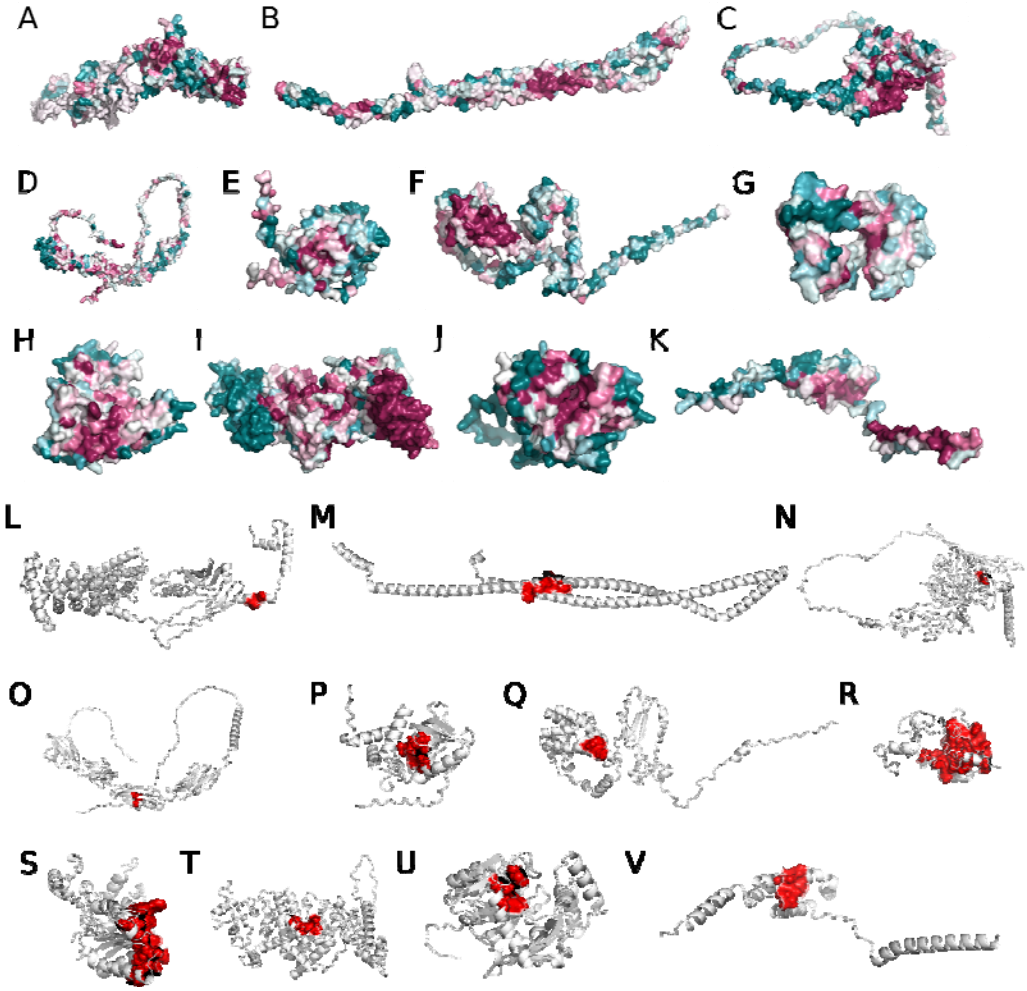

Figure 5. The best docking molecular for each protein. A. ARMCX5; B. CCDC; C. CDSN; D. CEACAM1; E. CHAC1; F. CIART; G. CIRP; H. NQO1; I. NR1D1; J. NUDT22; K. RAMP3.

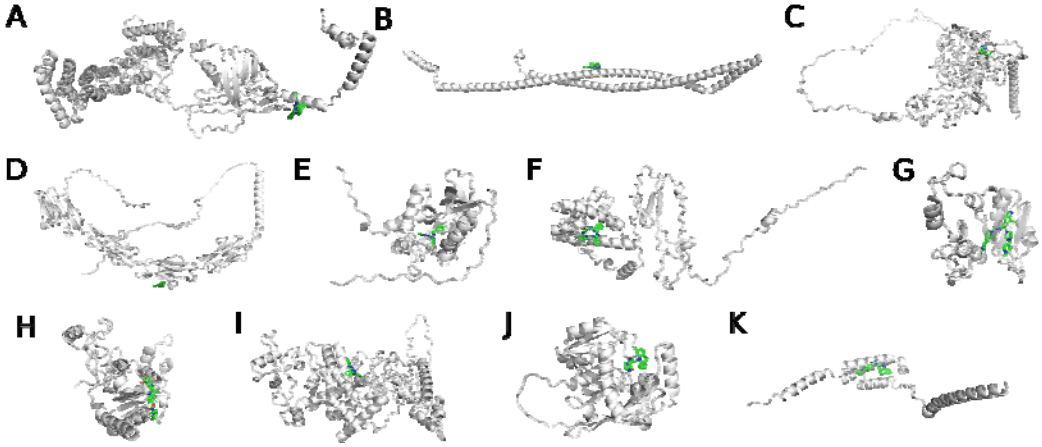

Figure 6. The RMSD and RMSF of MD simulation. A. The RMSD of proteins. B. The RMSF of proteins. C. The RMSD of each molecular of proteins.

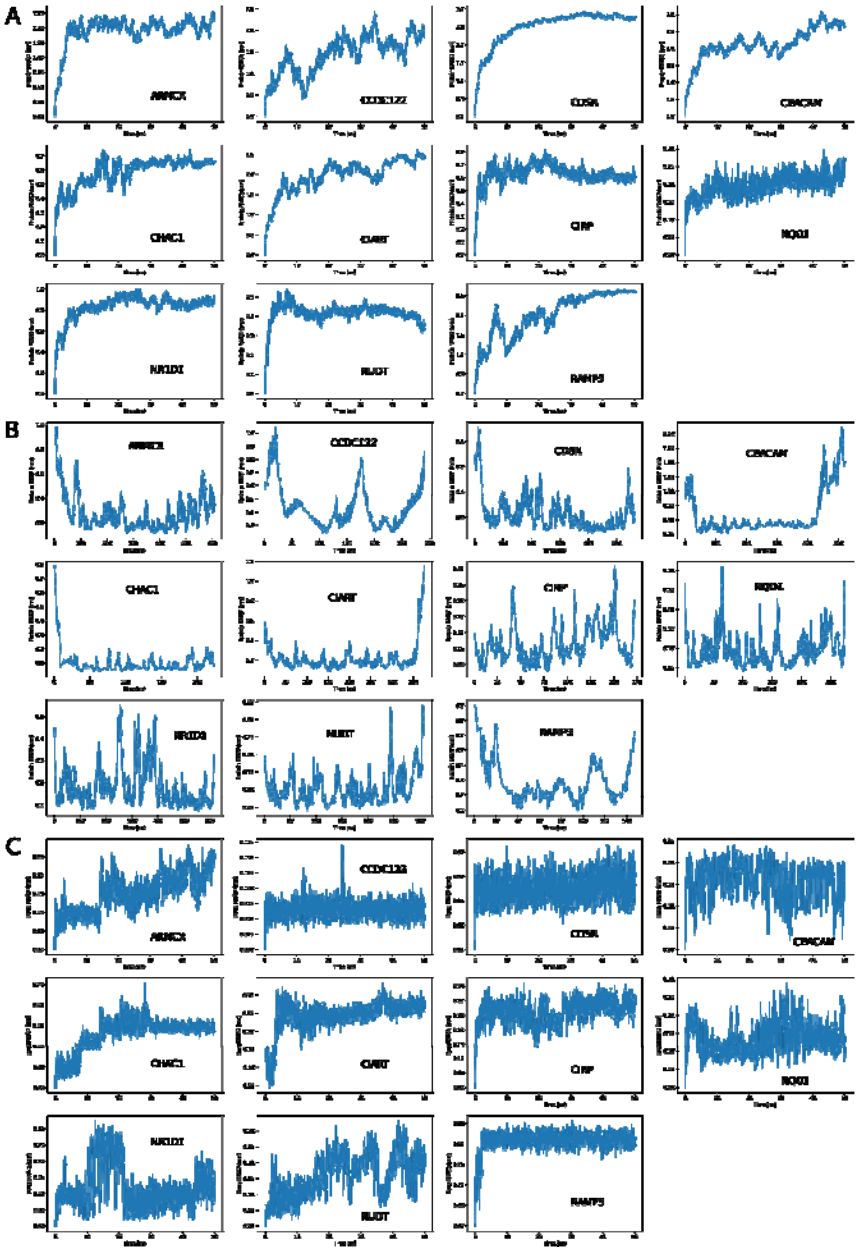

Bioinfo-pharmacology — a new pharmacology based on PageRank of multiple targets and multiple moleculars: an example of therapeutic hypothermia

Additional file

This appendix provides further methodological detail for "Bioinfo-pharmacology — a new pharmacology based on PageRank of multiple targets and multiple moleculars: an example of therapeutic hypothermia".

Table 1. The docking results of top 10 drugs for each protein.

Protein	Drug	affinity (kcal/mol)
nudt22	Mosapramine	-11.6
nudt22	Exicorilant	-11.1
nudt22	GSK2798745	-11
nudt22	Fluzoparib	-11
nudt22	Enzastaurin	-10.9
nudt22	Laniquidar	-10.9
nudt22	Tepotinib	-10.8
nudt22	Atogepant	-10.7
nudt22	Ubrogepant	-10.6
nudt22	Tirilazad	-10.6
ccdc122	Phthalocyanine	-9.1
ccdc122	Vazegepant	-8.6
ccdc122	Afoxolaner	-8.5
ccdc122	Tirilazad	-8.5
ccdc122	Dirlotapide	-8.4
ccdc122	Lifirafenib	-8.4
ccdc122	MK-0773	-8.4
ccdc122	Bemcentinib	-8.4
ccdc122	N-cyclopropyl-4-methyl-3-[1-(2-methylphenyl)phthalazin-6-yl]benzamide	-8.2
ccdc122	PF-5190457	-8.2
cdsn	Zoliflodacin	-10.6
cdsn	Fulacimstat	-9.5
cdsn	HQP1351	-9.2
cdsn	Atogepant	-9.2
cdsn	Vazegepant	-9.2
cdsn	Tarazepide	-9.1
cdsn	Rimegepant	-9.1
cdsn	Lifirafenib	-9.1
cdsn	Liafensine	-9
cdsn	Icotinib	-9
nr1d1	Phthalocyanine	-9
nr1d1	Tirilazad	-8.7

nr1d1	MK-0773	-8.7
nr1d1	Vazegepant	-8.5
nr1d1	TMC-647055	-8.5
nr1d1	Afoxolaner	-8.5
nr1d1	(20S)-19,20,21,22-TETRAHYDRO-19-OXO-5H-18,20-ETHANO-12,14-ETHENO-6,10-METHENO-18H-BENZ[D]IMIDAZO[4,3-K][1,6,9,12]OXATRIAZA-CYCLOOCTADECOSINE-9-CARBONITRILE	-8.5
nr1d1	Quarfloxin	-8.5
nr1d1	Beclabuvir	-8.4
nr1d1	1-(2,6-Dichlorophenyl)-5-(2,4-Difluorophenyl)-7-Piperidin-4-Yl-3,4-Dihydroquinolin-2(1h)-One	-8.4
nqo1	Irinotecan	-9.5
nqo1	Lifirafenib	-9.4
nqo1	Phthalocyanine	-9.4
nqo1	MK-3207	-9.4
nqo1	Tirilazad	-9.2
nqo1	Merestinib	-9.2
nqo1	Atogepant	-9
nqo1	Umbralisib	-9
nqo1	Gedatolisib	-9
nqo1	Ubrogepant	-8.9
ciart	Phthalocyanine	-8.2
ciart	Lumacaftor	-7.8
ciart	Rebastinib	-7.8
ciart	Bemcentinib	-7.7
ciart	Conivaptan	-7.6
ciart	MK-3207	-7.6
ciart	TMC-647055	-7.6
ciart	Quarfloxin	-7.6
ciart	Vazegepant	-7.6
ciart	Irinotecan	-7.6
cirp	Vazegepant	-10.6
cirp	MK-3207	-10.1
cirp	Lumacaftor	-10
cirp	Lifirafenib	-9.9
cirp	Phthalocyanine	-9.9
cirp	Atogepant	-9.9
cirp	Bemcentinib	-9.8
cirp	Rimegepant	-9.7
cirp	Ergotamine	-9.7
cirp	Galicaftor	-9.7
chac1	AC-430	-11.8
chac1	2'-deoxy-N-(naphthalen-1-ylmethyl)guanosine_5'-	-11.5

	(dihydrogen_phosphate)	
chac1	Glisoxepide	-11.4
chac1	Tioclomarol	-11.4
chac1	Vactosertib	-11.4
chac1	Raltegravir	-11.4
chac1	3-FLUORO-N-[1-(4-FLUOROPHENYL)-3-(2-THIENYL)-1H-PYRAZOL-5-YL]BENZENESULFONAMIDE	-11.1
chac1	BPN-14770	-11
chac1	Glipizide	-10.9
chac1	N,N'-DIPHENYLPYRAZOLO[1,5-A][1,3,5]TRIAZINE-2,4-DIAMINE	-10.8
ceacam1	Adapalene	-9.2
ceacam1	3-(2-AMINOQUINAZOLIN-6-YL)-4-METHYL-N-[3-(TRIFLUOROMETHYL)PHENYL]BENZAMIDE	-9
ceacam1	3-carboxamido-1,3,5(10)-estratrien-17(R)-spiro-2'(5',5'-dimethyl-6'oxo)tetrahydropyran	-8.9
ceacam1	Zk-806450	-8.8
ceacam1	CD564	-8.8
ceacam1	4-CHLORO-3',3"-DIBROMOPHENOL-1,8-NAPHTHALEIN	-8.7
ceacam1	Liafensine	-8.7
ceacam1	SR11254	-8.7
ceacam1	Arotinoid_acid	-8.6
ceacam1	[4-(5-naphthalen-2-yl-1H-pyrrolo[2,3-b]pyridin-3-yl)phenyl]acetic_acid	-8.6
ramp3	Bemcentinib	-7.5
ramp3	Phthalocyanine	-7.4
ramp3	TMC-647055	-7.2
ramp3	Tirilazad	-7
ramp3	Lorecivivint	-6.9
ramp3	3-(2-aminoquinazolin-6-yl)-1-(3,3-dimethylindolin-6-yl)-4-methylpyridin-2(1H)-one	-6.9
ramp3	Omaveloxolone	-6.7
ramp3	1-{4-[4-Amino-6-(4-methoxyphenyl)furo[2,3-d]pyrimidin-5-yl]phenyl}-3-[2-fluoro-5-(trifluoromethyl)phenyl]urea	-6.7
ramp3	Naldemedine	-6.7
ramp3	MK-0773	-6.7
armcx5	Phthalocyanine	-8.6
armcx5	Bemcentinib	-7.7
armcx5	MK-3207	-7.5
armcx5	Tirilazad	-7.5

armcx5	Tasosartan	-7.5
armcx5	2-(2f-Benzothiazolyl)-5-Styryl-3-(4f-Phthalhydrazidyl)Tetrazolium_Chloride	-7.4
armcx5	JNJ-40346527	-7.4
armcx5	Radotinib	-7.4
armcx5	LY-2623091	-7.3
armcx5	Ergotamine	-7.3

Table 2. Rank of 3 drug combinations of different group.

	drug1	drug2	drug3	value	persentage	value	persentage	value	persentage	personalized_weight_PageRank	Drug-protein-expression fit score
h0.5h	Lorecivivint	Vactosertib	Fluzoparib	0.31	33.33	0.31	33.19	0.31	33.47	0.92	2.58
	Lorecivivint	2'-deoxy-N-(naphthalen-1-ylmethyl)guanosine 5'-(dihydrogen phosphate)	Fluzoparib	0.31	33.31	0.31	33.24	0.31	33.45	0.92	2.58
	Lorecivivint	Fluzoparib	AC-430	0.31	33.37	0.31	33.53	0.31	33.10	0.92	2.59
h1h	Lorecivivint	Raltegravir	AC-430	0.31	33.32	0.31	33.22	0.31	33.46	0.93	4.99
	Lorecivivint	Vactosertib	AC-430	0.31	33.33	0.31	33.19	0.31	33.48	0.93	4.97

	Glisoxepide	Lorecivivint	AC-430	0.31	33.11	0.31	33.38	0.31	33.52	0.93	4.95
h2h	Phthalocyanine	Bemcentinib	Vazegepant	0.32	33.89	0.31	32.95	0.31	33.16	0.93	5.32
	Phthalocyanine	Lifirafenib	Vazegepant	0.32	33.97	0.31	32.80	0.31	33.23	0.93	5.28
	Phthalocyanine	Vazegepant	Tirilazad	0.32	33.99	0.31	33.28	0.31	32.73	0.93	5.31
h4h	Adapalene	3-(2-AMINOQUINAZOLIN-6-YL)-4-METHYL-N-[3-(TRIFLUOROMETHYL)PHENYL]BENZAMIDE	CD564	0.31	33.35	0.31	33.39	0.31	33.26	0.93	1.81
	Adapalene	3-(2-	Phthalocy	0.31	33.39	0.31	33.43	0.31	33.18	0.93	1.81

		AMINOQUINAZOLIN-6-YL)-4-METHYL-N-[3-(TRIFLUOROMETHYL)PHENYL]BENZAMIDE	anine								
	3-(2-AMINOQUINAZOLIN-6-YL)-4-METHYL-N-[3-(TRIFLUOROMETHYL)PHENYL]BENZAMIDE	Phthalocyanine	CD564	0.31	33.47	0.31	33.20	0.31	33.33	0.93	1.81
	Phthalocyanine	Lifirafenib	MK-3207	0.30	33.36	0.30	33.22	0.30	33.42	0.90	4.27
h8h	Phthalocyanine	MK-3207	Vazegepant	0.30	33.39	0.30	33.45	0.30	33.15	0.90	4.29
	Phthalocyanine	Lifirafenib	Vazegepan	0.30	33.46	0.30	33.32	0.30	33.22	0.90	4.29

			t								
	Phthalocyanine	Lifirafenib	MK-3207	0.30	33.35	0.30	33.22	0.30	33.43	0.89	5.33
h18	Phthalocyanine	MK-3207	Vazegepant	0.30	33.43	0.30	33.50	0.30	33.06	0.89	5.36
h	Phthalocyanine	Lifirafenib	Vazegepant	0.30	33.50	0.30	33.37	0.30	33.13	0.89	5.35